Dysregulation of ADAM10 shedding activity as a mechanism of cancer resistance in the naked mole-rat

Paulina Urriola-Muñoz*[1], Luke A. Pattison[1], Ewan St. John. Smith*[1]

[1]Department of Pharmacology, University of Cambridge, Cambridge, CB2 1PD, UK

*Corresponding authors:

Paulina Urriola-Muñoz, pau20@cam.ac.uk

Ewan St. John Smith, es336@cam.ac.uk

Abstract

The naked mole-rat (NMR, *Heterocephalus glaber*) is of significant interest to biogerontological research, rarely developing age-associated diseases, such as cancer. The transmembrane glycoprotein CD44 is upregulated in certain cancers and CD44 cleavage by a disintegrin and metalloproteinase 10 (ADAM10) regulates cellular migration. Here we provide evidence that altered CD44 signalling may be involved in NMR cancer resistance. Although mature ADAM10 is expressed in primary NMR skin fibroblasts, and ionomycin increases cell surface ADAM10 localization, we observed an absence of endogenous CD44 shedding, as well as of exogenous and overexpressed betacellulin, whereas ionomycin induced ADAM10-dependent cleavage of CD44 and betacellulin in mouse primary skin fibroblasts. Overexpressing a hyperactive form of the Ca^{2+}-dependent phospholipid scramblase ANO6 in NMR primary skin fibroblasts increased phosphatidylserine externalization, rescuing the ADAM10 sheddase activity and promoting wound closure. These findings suggest that dysregulation of ADAM10 shedding activity may contribute to the NMR's cancer resistance.

Keywords: Naked mole-rat, ADAM10, CD44, ANO6, cancer

Introduction

The naked mole-rat (NMR, *Heterocephalus glaber*) is a eusocial mammal with an exceptionally long lifespan of 35+ years, compared with sized rodents (Holmes and Goldman, 2021; Ruby et al., 2018). Moreover, NMRs rarely develop age-associated diseases, such as cancer (Buffenstein et al., 2022; Hadi et al., 2021), which is why NMRs are recognized as species of particular biogerontological interest (Buffenstein, 2005; Edrey et al., 2011). However, what determines many aspects of the healthy ageing of the NMR is currently unknown.

There are several mechanisms that might contribute to the low incidence of cancer in NMRs, including a slow somatic mutation rate (Cagan et al., 2022) and altered CD44 signalling (Keane et al., 2014; Tian et al., 2013); the concept that NMR cells do not undergo oncogenic transformation has been refuted (Hadi et al., 2020). CD44 is a widely expressed, type I non-kinase transmembrane receptor for various extracellular matrix components, including hyaluronan, collagen, chondroitin sulphate, laminin and fibronectin (Banerji et al., 2007; Chen et al., 2020; Ishii et al., 1993; Jalkanen and Jalkanen, 1992; Radotra et al., 1994). CD44 plays a role in numerous physiological and pathological processes, such as cellular adhesion, angiogenesis, metastasis, migration, and invasion (Bourguignon, 2008; Ludwig et al., 2019; Wang et al., 2019b; Wolf et al., 2020; Yae et al., 2012; Zoller, 1995). In addition, CD44 has been associated with cancer progression, being one of the most consistent markers of cancer stem cells and involved in their generation, maintenance, and survival (Corte et al., 2010; Hassn Mesrati et al., 2021; Leung et al., 2010; Lokeshwar et al., 1995; Olsson et al., 2011; Takaishi et al., 2009; Zoller, 2011).

The principal domains of CD44 are the extracellular domain or ectodomain, the transmembrane domain, and the intracellular/cytoplasmic domain (Lesley and Hyman, 1998). CD44 can be cleaved in the ectodomain by metalloproteases (Nagano et al., 2004; Nagano and Saya, 2004; Nakamura et al., 2004), a process stimulated by extracellular Ca^{2+} influx, the activation of Rho family small GTPases, Rac and Ras oncoproteins, and the activation of protein kinase C (Kawano et al., 2000; Nagano et al., 2004; Okamoto et al., 1999a). Cleavage of the CD44 ectodomain is highly prevalent in patients with tumours including glioma, breast, lung, colon and ovarian cancers (Okamoto et al., 2002; Yamane et al., 1999), and high levels of soluble CD44 have been found in the serum of patients with cancer (Guo et al., 1994; Masson et al., 1999). Furthermore, CD44 cleavage promotes tumour cell migration (Kawano et al., 2000; Kolliopoulos et al., 2021; Kung et al., 2012; Sugahara et al., 2003). Therefore, it is clear that CD44 cleavage plays an important role in tumour progression.

A Disintegrin and Metalloprotease 10 (ADAM10) is one of the metalloproteases involved in CD44 cleavage (Anderegg et al., 2009; Murai et al., 2006; Nagano et al., 2004; Pan et al., 2012). ADAM proteins are type I metalloproteases responsible for the shedding of different membrane-bound receptors and ligands controlling many cellular functions (Reiss and Saftig, 2009). Among the ADAM family, ADAM10 is one of best characterized members, being able to cleave many proteins, including CD44, betacellulin (BTC), Notch and N-cadherin (Hartmann et al., 2002; Maretzky et al., 2005; Nagano et al., 2004; Sahin et al., 2004), and also being involved in diverse physiological processes, such as fertilization, neurogenesis and angiogenesis (Reiss et al., 2005; Sahin et al., 2004). Dysregulation of ADAM10 activity is associated with different pathologies, such as embryonic lethality in mice

due to disturbed Notch signalling being caused by depletion of the ADAM10 gene (Hartmann et al., 2002) and upregulation of ADAM10 occurring in melanoma (Lee et al., 2010), as well as roles for dysregulation of ADAM10 shedding activity occurring in Alzheimer's disease, and cancer development (Marcello et al., 2017; Murphy, 2008; Weskamp et al., 2006).

It is well known that the constitutive shedding activity of ADAM10 is enhanced by Ca^{2+} influx, which can be induced by ionophores as ionomycin (IM) (Maretzky et al., 2005; Reiss and Bhakdi, 2012). Recently, it has also been shown that exposure of the negatively charged phosphatidylserine (PS) in the outer leaflet of the cell membrane regulates substrate cleavage by ADAM10 (Bleibaum et al., 2019).

Considering what is understood about the role of ADAM10/CD44 in cellular function, we hypothesize that another mechanism that might contribute to the NMR's cancer resistance would be dysregulation of CD44 cleavage by ADAM10. Experiments conducted in NMR primary skin fibroblasts indicated an absence of CD44 cleavage in NMR cells induced by IM. Furthermore, in NMR fibroblasts, ADAM10 is expressed as pro- and mature form, and although IM induced the translocation of ADAM10 to the cell membrane of NMR fibroblasts, it does not induce increased ADAM10-dependent shedding of the ADAM10 substrate BTC when is overexpressed. However, when NMR primary skin fibroblasts overexpressed a hyperactive form of ANO6 (ANO6-HA), a Ca^{2+}-dependent phospholipid scramblase, an increase of the PS externalization was observed, and IM was now able to induce ADAM10-dependent BTC shedding. Finally, ANO6-HA overexpression promoted wound closure. All these data suggest that the dysregulation of ADAM10 shedding activity may contribute to NMR's cancer resistance.

Results

CD44 cleavage is not induced by IM in NMR primary skin fibroblasts

CD44 cleavage by metalloproteases has been implicated in cancer cell migration (Kolliopoulos et al., 2021; Nagano et al., 2004; Nakamura et al., 2004; Okamoto et al., 1999b) and cancer resistance is a characteristic of the naked mole-rat (NMR) biology (Hadi et al., 2021). We therefore used immunoblotting to analyse the extent of IM-induced CD44 cleavage by A Disintegrin and Metalloprotease 10 (ADAM10) in NMR primary skin fibroblasts (NPSF) and mouse primary skin fibroblasts (MPSF); IM is a well characterised initiator of Ca^{2+} influx that activates ADAM10 sheddase function (Maretzky et al., 2015).

In all conditions, cells were preincubated for 30 min with the proteasomal inhibitor MG132 (10 µM) to prevent degradation of CD44 cleavage products (Okamoto et al., 2001). In MPSF it was observed that the CD44 full length protein has a molecular weight of ~100 kDa, which is comparable to that previously published (Kolliopoulos et al., 2021; Okamoto et al., 1999b). After treatment for 1 h with 0.5 µM IM, an increase in the density of two fragments between ~15 and ~25 kDa was observed. To determine the participation of metalloproteases, and specifically ADAM10 in this process, the effects of the following drugs was observed: batimastat, a general metalloprotease inhibitor (BB-94, 10 µM), GW280264X, an inhibitor of ADAM10/ADAM17 (GW, 1 µM) and GI254023X, which is selective for ADAM10 (GI, 1µM) (Ludwig et al., 2005). In MPSF, all three inhibitors prevented IM-induced CD44 cleavage

(Figure 1A), suggesting a key role for ADAM10 in CD44 cleavage in MPSF. However, in NPSF IM failed to induce CD44 cleavage (Figure 1B). These data show for first time that CD44 cleavage is not induced by IM in NPSF.

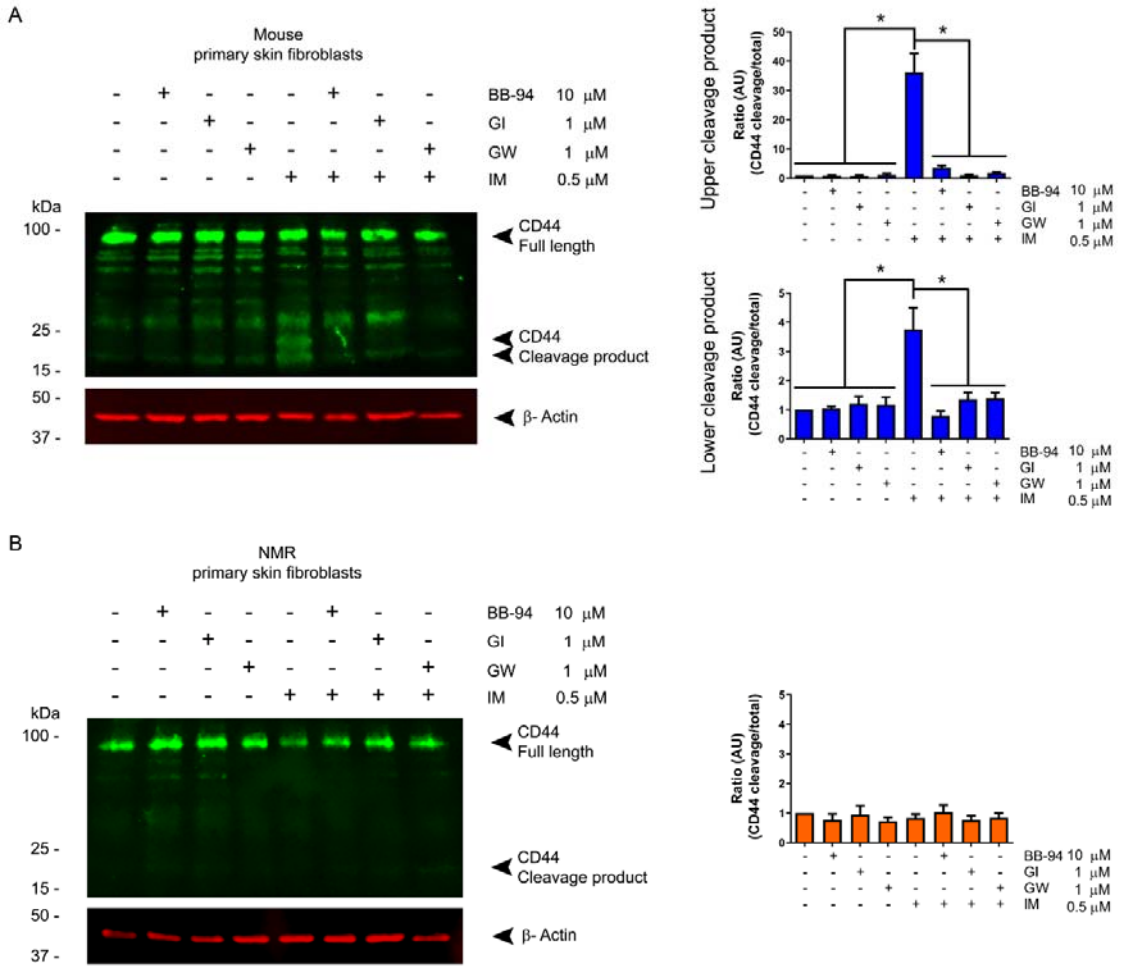

Figure 1: CD44 cleavage is not induced by IM in NMR primary skin fibroblasts

An immunoblot was performed to evaluate the full length and cleaved products of CD44 in (A) MPSF and (B) NPSF. Cells were treated for 30 min with a general inhibitor of metalloproteases (Batimastat, BB, 10 µM), an ADAM10 inhibitor (GI254023X, GI, 1 µM) or an ADAM10/ADAM17 inhibitor (GW280264X, GW, 1 µM), before stimulating cells for 1 h with ionomycin (IM, 0.5 µM). (A) In MPSF, the full CD44 protein has a molecular weight of around ~100 kDa, when CD44 is cleaved, two fragments between ~15 and ~25 kDa are produced. Comparison of the upper and lower cleavage products with the full protein levels generated a ratio of CD44 cleavage/total. (B) In NPSF, the full CD44 protein has a molecular weight of around ~100 kDa, when CD44 is cleaved, only one fragment around ~15 kDa was observed. Comparison of the cleavage product with the full protein levels generated a ratio of CD44 cleavage/total. Vehicle: DMSO. Results are mean ± SEM; n=3. For statistical

analysis mean values were compared using an ANOVA and Tukey's post-hoc test; *p ≤ 0.05.

NMR primary skin fibroblasts express ADAM10, which undergoes cell membrane translocation, but is not activated by IM

To determine if the lack of IM-induced CD44 cleavage in NPSF is due to these cells not expressing ADAM10, we compared ADAM10 expression with MPSF by immunoblotting. We observed that pro- and mature ADAM10 are expressed in both MPSF and NPSF, higher levels of pro ADAM10 being expressed in NPSF compared to MPSF, but no difference was found in expression of mature ADAM10 between fibroblasts of different species (Figure 2A). Because CD44 cleavage takes place at the cell surface, we next evaluated if IM could induce ADAM10 cell membrane translocation. MPSF and NPSF were treated for 1 h with IM 0.5 µM and the surface localisation of ADAM10 was evaluated by biotinylation of cell membrane proteins. An increase in mature ADAM10 protein levels was found in both MPSF and NPSF, treated with IM compared with the vehicle in the biotinylated fraction, with no changes in the mature ADAM10 protein levels in the total fraction (Figure 2B). These results were confirmed with immunostaining of ADAM10 in MPSF and NPSF. Localisation of ADAM10 (green) closer to the cell membrane (wheat germ agglutin, magenta) was observed when both, MPSF and NPSF, were treated for 1 h with IM 0.5 µM (Figure 2C). These results suggest that IM induces the translocation of ADAM10 to the cell surface in both MPSF and NPSF. Finally, to evaluate the ADAM10 shedding activity, more broadly MPSF and NPSF were transfected with the alkaline phosphatase (AP)-tagged ADAM10 substrate betacellulin (BTC) (Sahin et al., 2004). A significative increase in the shedding of BTC after 1 h of incubation with IM 0.5 µM was observed in MPSF, which was prevented with the batimastat (BB-94, 10 µM), GI254023X (GI, 1 µM), and GW280264X (GW, 1 µM) inhibitors (Figure 2D), suggesting that ADAM10 participates in the IM-induced BTC shedding in MPSF. However, IM does not induce BTC shedding in NPSF (Figure 2D). Therefore, using two different approaches, evaluating the cleavage of an endogenous substrate, CD44 (Figure 1B) or the shedding of an exogenous and well-studied substrate, BTC (Figure 2D), it is clear that IM does not induced ADAM10-dependent shedding activity in NPSF.

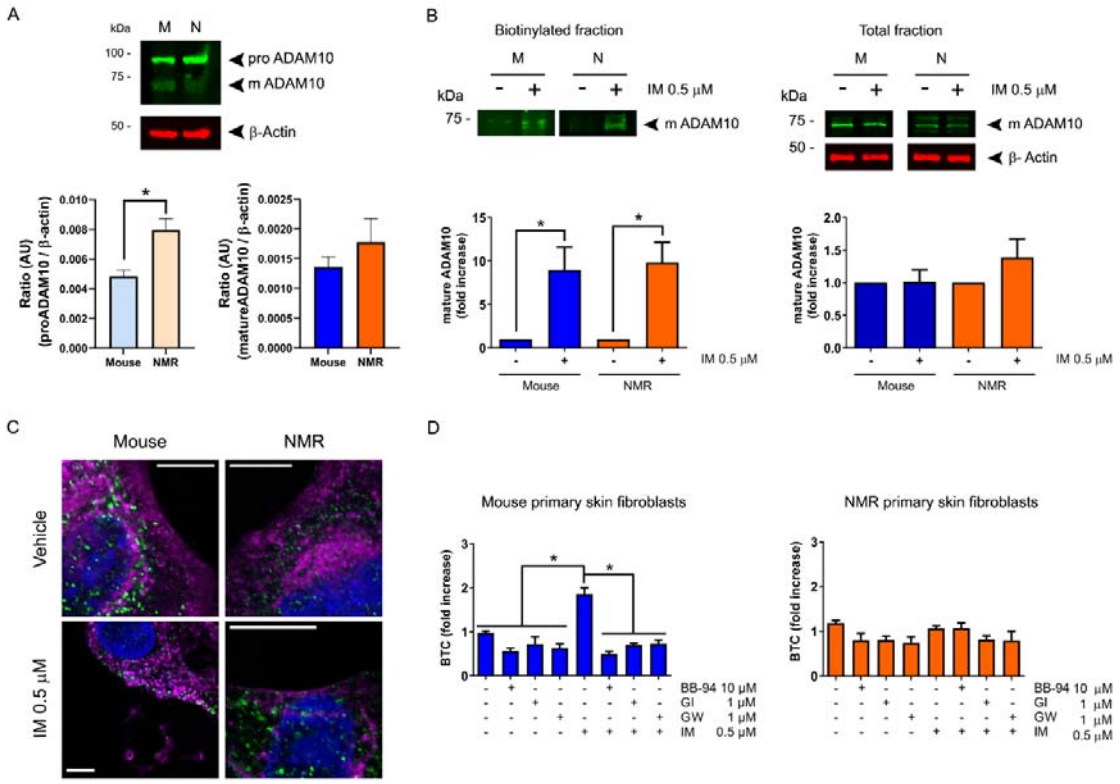

Figure 2: NMR primary skin fibroblasts express ADAM10, which undergoes cell membrane translocation, but is not activated by IM

(A) Immunoblot of ADAM10, where pro- and mature forms were observed in MPSF and NPSF. β-actin was used as loading control. Results are mean ± SEM; n=3. For statistical analysis, mean values were compared using an unpaired t test; *p ≤ 0.05.

(B) Immunoblot of mature cell surface and total protein fraction ADAM10 in MPSF and NPSF treated for 1 h with ionomycin (IM, 0.5 μM). β-actin was used as loading control in the total protein fraction. Results are mean ± SEM; n=3. For statistical analysis, mean values were compared using an unpaired t test; *p ≤ 0.05.

(C) Pseudocoluor; ADAM10 (green), wheat germ agglutinin (magenta) and NucRed™ Live 647 (blue) staining in MPSF and NPSF, with or without a treatment for 1 h with ionomycin (IM, 0.5 μM). Vehicle: DMSO. Scale bar: 10 μm.

(D) MPSF and NPSF were transfected with the AP-tagged ADAM10 substrate BTC. BTC shedding was evaluated after cells were treated for 30 min with a general inhibitor of metalloproteases (Batimastat, BB, 10 μM), an ADAM10 inhibitor (GI254023X, GI, 1 μM) or an ADAM10/ADAM17 inhibitor (GW280264X, GW, 1 μM), and then cells were stimulated for 1 h with ionomycin (IM, 0.5 μM). Vehicle: DMSO. Results are mean ± SEM; n=3. For statistical analysis, mean values were compared using an ANOVA and Tukey's post-hoc test; *p ≤ 0.05.

IM induces CD44 cleavage and ADAM10 shedding activity in both mouse and NMR SV40-Ras skin fibroblasts

To determine if the absence of IM-induced ADAM10 shedding activity is a general phenomenon of NMR cells, or one that is restricted to primary cells, oncogenic mouse and NMR SV40-Ras skin fibroblasts that were previously developed in our lab (Hadi et al., 2020) were used. Firstly, IM-induced CD44 cleaved protein levels were determined by immunoblot. As previously described for primary cells, in all the conditions the cells were preincubated for 30 min with the proteasomal inhibitor MG132 (10 µM) to prevent the degradation of CD44 cleavage products (Okamoto et al., 2001). In both mouse and NMR SV40-Ras skin fibroblasts, after treatment for 10 min with IM 2.5 µM, a significant increase of two fragments between ~15 and ~25 kDa were observed, which was prevented with the use of batimastat (BB-94, 10 µM), GI254023X (GI, 1 µM), GW280264X (GW, 1 µM) inhibitors (Figure 3A and 3B), suggesting that ADAM10 participates in IM-induced CD44 cleavage in mouse and NMR SV40-Ras cells. In addition, pro- and mature ADAM10 is expressed in both, mouse and NMR SV40-Ras skin fibroblasts, with higher pro-ADAM10 levels in mouse compared to NMR cells, but there was no difference regarding levels of mature ADAM10 between the cells from mouse or NMR (Figure S1A). An IM-induced increase in mature ADAM10 was found in both mouse and NMR SV40-Ras skin fibroblasts compared to vehicle in the biotinylated cell membrane protein fraction, with no change detected in the total fraction (Figure S1B). A significative increase in the shedding of BTC after 10 min of incubation with IM 2.5 µM was observed in both, mouse and NMR SV40-Ras skin fibroblasts transfected with the AP-tagged ADAM10 substrate BTC. This increase was prevented with the batimastat (BB-94, 10 µM), GI254023X (GI, 1 µM), and GW280264X (GW, 1 µM) inhibitors (Figure 3C and 3D). These data suggest that IM activated the shedding activity of ADAM10, inducing ADAM10-dependent CD44 cleavage and BTC shedding in oncogenic cells from both mouse and NMR.

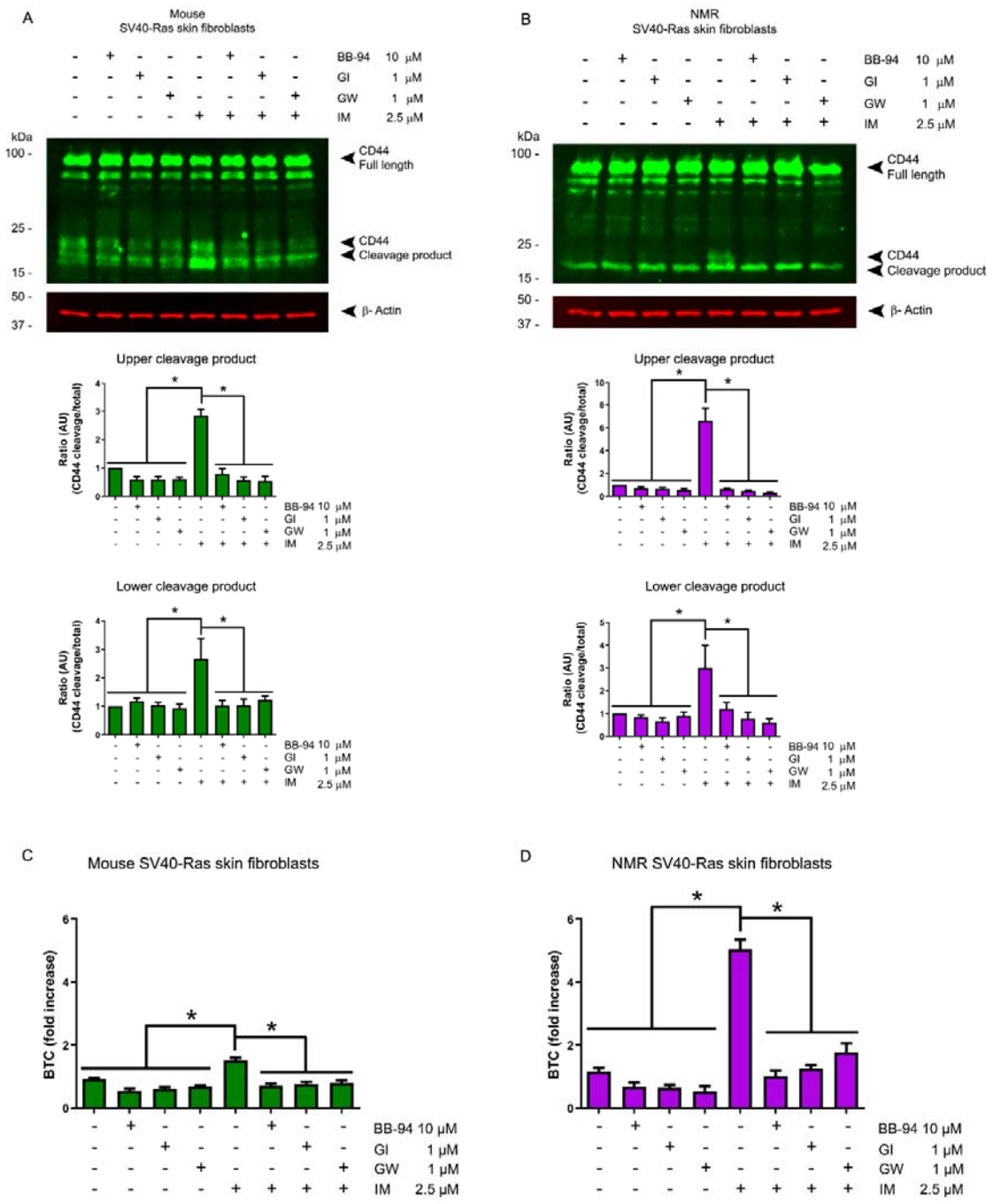

Figure 3: IM induces CD44 cleavage and ADAM10 shedding activity in both mouse and NMR SV40-Ras skin fibroblasts

Immunoblot evaluation of full length and cleavage products of CD44 in (A) mouse and (B) NMR SV40-Ras skin fibroblasts. Cells were treated for 30 min with a general inhibitor of metalloproteases (Batimastat, BB, 10 µM), an ADAM10 inhibitor (GI254023X, GI, 1 µM) or an ADAM10/ADAM17 inhibitor (GW280264X, GW, 1 µM), before stimulating cells for 10 min with ionomycin (IM, 2.5 µM). Full CD44 protein has a molecular weight of around ~100 kDa, when CD44 is cleaved, two fragments between ~15 and ~25 kDa are produced. The upper and lower cleavage product is compared with the full protein levels to generate a ratio of CD44 cleavage/total. β-actin was used as loading control. Vehicle: DMSO. Results are mean ± SEM; n=3. For statistical analysis, mean values were compared using an ANOVA and Tukey's post-hoc test; *$p \leq 0.05$.

(C) Mouse and (D) NMR SV40-Ras skin fibroblasts were transfected with the AP-tagged ADAM10 substrate BTC. BTC shedding was evaluated after cells were treated for 30 min with a general inhibitor of metalloproteases (Batimastat, BB, 10 µM), an ADAM10 inhibitor (GI254023X, GI, 1 µM) or an ADAM10/ADAM17 inhibitor (GW280264X, GW, 1 µM), and then cells were stimulated for 10 min with IM, 2.5 µM. Vehicle: DMSO. Results are mean ± SEM; n=3. For statistical analysis, mean values were compared using an ANOVA and Tukey's post-hoc test; *$p \leq 0.05$.

NMR SV40-Ras skin fibroblasts have more phosphatidylserine in the outer leaflet of the cell membrane

To try to elucidate why in NPSF the shedding activity of ADAM10 is not induced by IM but it is in NMR SV40-Ras skin fibroblasts, the localisation of the phospholipid phosphatidylserine (PS) in the outer leaflet of the cell membrane was evaluated. This is because surface exposure of negatively charged PS on the cell membrane has been proposed to regulate ADAM10 shedding activity (Bleibaum et al., 2019). Using the RealTime-Glo™ Annexin V luminescence assay, the binding of annexin V with PS in the outer leaflet of the cell membrane was measured, providing a readout in relative luminescence units (RLU). Simultaneous staining of the nucleus with the NucRed™ Live 647 ReadyProbes® reagent provided a readout of relative fluorescence units (RFU), indicative of the number of cells. The ratio of both parameters was determined in MPSF, NPSF, mouse and NMR SV40-Ras skin fibroblasts (Figure 4A). No differences were found in the PS exposure to the outer leaflet in mouse primary versus SV40-Ras cells, however, a higher levels of PS was found in the NMR SV40-Ras cells compared with the primary cells (Figure 4B). This difference in the levels of PS in the outer leaflet of the cell membrane could explain why IM-induced ADAM10 shedding was observed in NMR SV40-Ras, but not in primary skin fibroblasts.

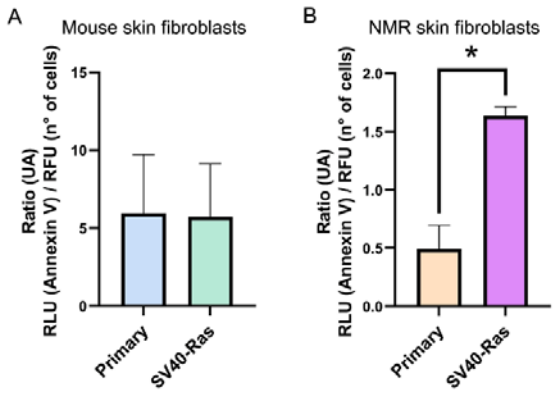

Figure 4: NMR SV40-Ras skin fibroblasts have more phosphatidylserine in the outer leaflet of their cell membranes

PS in the outer leaflet of the cell membrane was evaluated through the ratio of Annexin V (RLU) and n° of cells (RFU) in (A) mouse and (B) NMR primary and SV40-Ras skin fibroblasts. Results are mean ± SEM; n=3. For statistical analysis, mean values were compared using an unpaired t test; *p ≤ 0.05.

Overexpression of ANO6-HA rescues IM-induced ADAM10 shedding activity in NMR primary skin fibroblasts

To test whether inducing an increase of PS in the outer leaflet of the cell membrane could result in IM-induced ADAM10 shedding activity, MPSF and NPSF were transfected with either a hyperactive form of ANO6 (ANO6-HA) or GFP as a control. ANO6, is a Ca^{2+}-dependent phospholipid scramblase that increases PS externalization and ADAM10-dependent substrate shedding in COS7 cells (Bleibaum et al., 2019). 24 h post-transfection, an increase in ANO6 protein levels was observed in both MPSF and NPSF as evaluated by immunoblotting (Figure 5A and 5D). Concomitant with the ANO6 increase was observed an increase in the amount of PS in the outer leaflet of the cell membrane, again in both MPSF and NPSF (Figure 5B and 5E). Next, MPSF and NPSF were cotransfected with AP-tagged BTC and ANO6-HA (or GFP as control) for 24 h before evaluating ADAM10 shedding activity. As expected, treatment for 1 h with IM 0.5 µM induced an increase in the BTC shedding in both control and ANO6-HA MPSF, which was inhibited with both batimastat (BB, 10 µM) and GI254023X (GI, 1 µM); IM-induced BTC shedding was higher in cells overexpressing ANO6-HA (Figure 5C). Furthermore, as shown previously (Figure 2D), in NPSF cotransfected with AP-tagged BTC and GFP, IM 0.5 µM did not induce BTC shedding, however, in cells cotransfected with AP-tagged BTC and ANO6-HA, IM did induce BTC shedding, which is inhibited by both batimastat (BB, 10 µM) and GI254023X (GI, 1 µM) (Figure 5F). Due to NPSF not surviving at 37 ºC (Omerbasic et al., 2016), it is necessary for them to be maintained at 32°C under hypoxic conditions (5% CO_2 and 3% O_2), we thus considered if the difference in culturing conditions could explain the absence of IM-induced ADAM10 shedding activity in NPSF. Therefore, we performed the same experiments with MPSF cultured in the same conditions as NPSF. An increase of PS in the outer leaflet of the cell membrane was found in 32ºC MPSF transfected with the ANO6-HA compared with

control (Supplementary Figure 2A). Also, in 32ºC MPSF cotransfected with AP-tagged BTC and ANO6-HA (or GFP as control), IM 0.5 µM for 1 h induced an increase in the BTC shedding, with IM-induced BTC shedding being higher in cells overexpressing ANO6-HA compared to GFP expressing cells (Figure S2B). Taken together, these results demonstrate NMR ADAM10 is a functional metalloprotease and that the lower levels of PS in the outer leaflet of the cell membrane, rather than the lower temperature or percentage oxygen in which they are cultured, is responsible for the lack of IM-induced ADAM10 shedding activity in NPSF.

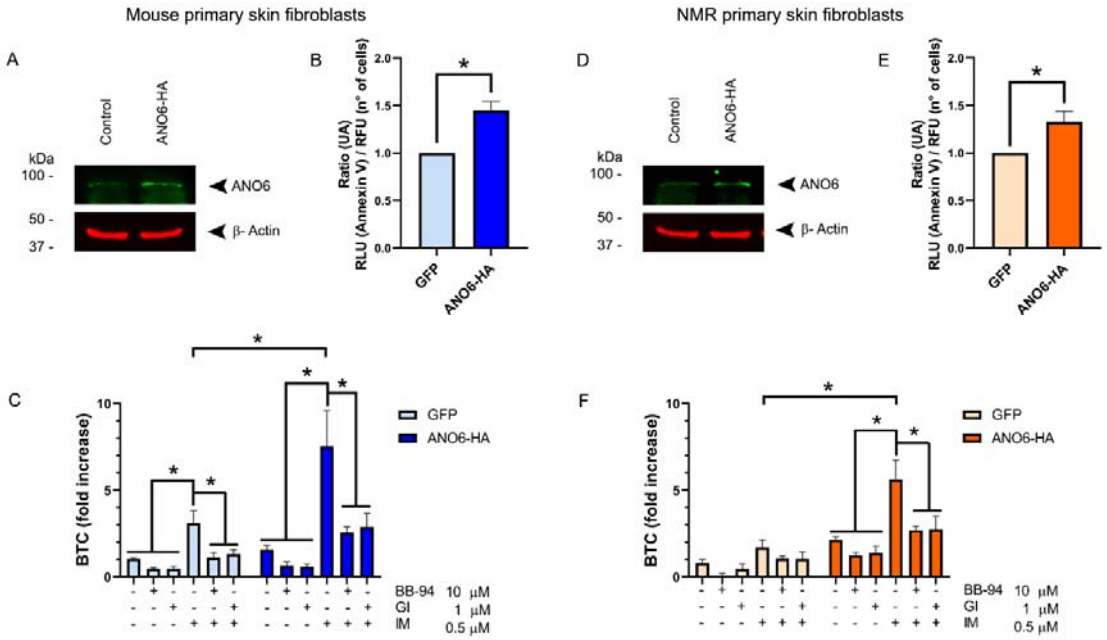

Figure 5: Overexpression of ANO6-HA rescues IM-induced ADAM10 shedding activity in NMR primary skin fibroblasts

Immunoblot of ANO6 in untransfected and ANO6 hyperactive (ANO6-HA) transfected (A) MPSF and (D) NPSF. β-actin was used as loading control. PS in the outer leaflet of the cell membrane was evaluated through the ratio between the Annexin V (RLU) and n° of cells (RFU) in cells transfected with ANO6-HA or GFP, as a control, in (B) mouse and (E) NMR primary skin fibroblasts. Results are mean ± SEM; n=4. For statistical analysis, mean values were compared using an unpaired t test; *p ≤ 0.05. (C) MPSF and (F) NPSF were cotransfected with the AP-tagged ADAM10 substrate BTC and ANO6-HA or GFP. BTC shedding was evaluated after cells were treated for 30 min with a general inhibitor of metalloproteases (Batimastat, BB, 10 µM) or the ADAM10 inhibitor (GI254023X, GI, 1 µM), and then cells were stimulated for 1 h with ionomycin (IM, 0.5 µM). Vehicle: DMSO. Results are mean ± SEM; n=4 for MPSF and n=3 for NPSF. For statistical analysis, mean values were compared using an ANOVA and Tukey's post-hoc test; *p ≤ 0.05.

Overexpression of ANO6-HA enhances migration of mouse and NMR primary skin fibroblasts

Migration of tumour cells in the extracellular matrix is necessary for tumour-cell invasion and metastasis. Different studies have shown that CD44 signalling is involved in cell migration in different cells models, including glioma cells (Koochekpour et al., 1995), human ovarian carcinoma SK-OV-3 cells (Bourguignon et al., 2007), and several breast cancer cell lines, including MDA-MB-231, MDA-MB-435, MDA-MB-468, T47D, and MCF-7 (Zen et al., 2008). In addition, the extracellular cleavage of CD44 promotes migration in different models such as, the pancreatic tumour cell line, MIA PaCa-2 (Kajita et al., 2001), human lung adenocarcinoma A549 cells (Kolliopoulos et al., 2021), and the human breast carcinoma cell lines, MDA-MB-435s and MDA-MB-231 (Kung et al., 2012). Interestingly, CD44 can induce its own cleavage by ADAM10 through activating the Rac pathway, as demonstrated in migration studies using the glioblastoma cell line, U251MG (Murai et al., 2004) and the human lung adenocarcinoma A549 cells (Kolliopoulos et al., 2021). Therefore, it was next evaluated if overexpression of ANO6-HA in MPSF and NPSF could induce migration. MPSF and NPSF were seeded and transfected in a dish with a silicone insert. After 24h the insert was removed to create a gap or “wound” and images were taken at 0, 3, 6, 9, 12, 24, 36 and 48 h to measure the percentage of wound closure. Both, MPSF and NPSD displayed an increased percentage of wound closure when transfected with ANO6-HA compared to cells transfect with GFP as a control (Figure 6A and 6B). Again, to determinate if culturing conditions could influence the migration assay, the same experiment was performed in MPSF cultured at 32°C and hypoxic conditions, and as expected, overexpression ANO6-HA induced an increase in the wound closure percentage (Figure S3).

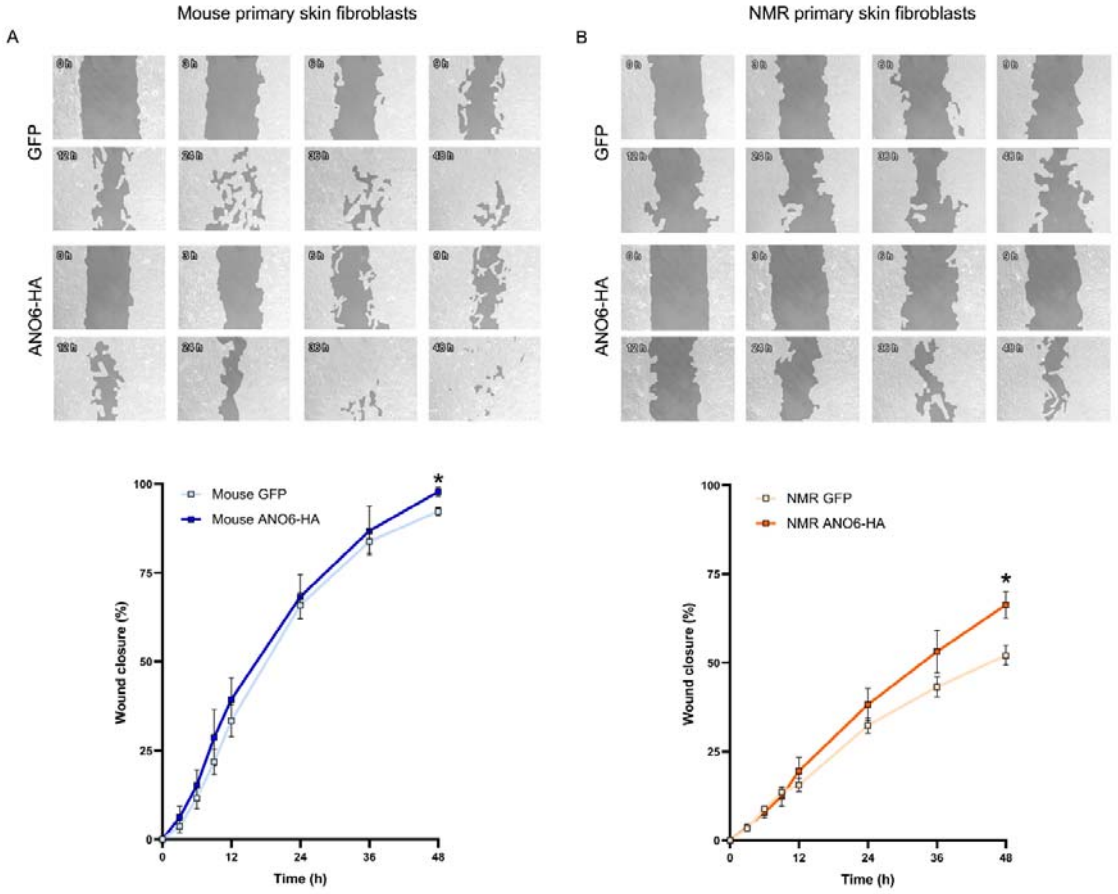

Figure 6: Overexpression of ANO6-HA enhances migration of mouse and NMR primary skin fibroblasts

(A) MPSF and (B) NPSF were transfected with ANO6-HA or GFP. Images were taken at 0, 3, 6, 9,12, 24, 36, and 48 h after removal of the silicone insert for gap creation. Quantification of the wound closure over the time is showed. Results are mean ± SEM; n=4 for MPSF and n=3 for NPSF. For statistical analysis, mean values were compared using an unpaired t test; *p ≤ 0.05.

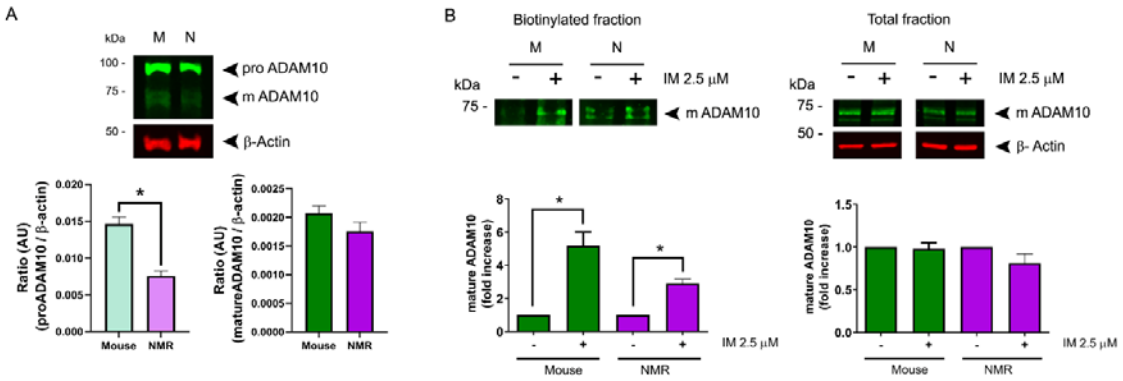

Supplementary Figure 1: Mouse and NMR SV40-Ras skin fibroblasts express ADAM10, which undergoes IM-induced translocated to the cell membrane

(A) Immunoblot of ADAM10, where pro- and mature forms were observed in mouse and NMR SV40-Ras skin fibroblasts. β-actin was used as loading control. Results are mean ± SEM; n=3. For statistical analysis, mean values were compared using an unpaired t test; *p ≤ 0.05.

(B) Immunoblot of mature ADAM10, comparing the biotinylated protein from the cell surface membrane fraction and total protein fraction in mouse and NMR SV40-Ras skin fibroblasts treated for 10 min with ionomycin (IM, 2.5 μM). β-actin was used as loading control in the total protein fraction. Results are mean ± SEM; n=3. For statistical analysis, mean values were compared using an unpaired t test; *p ≤ 0.05.

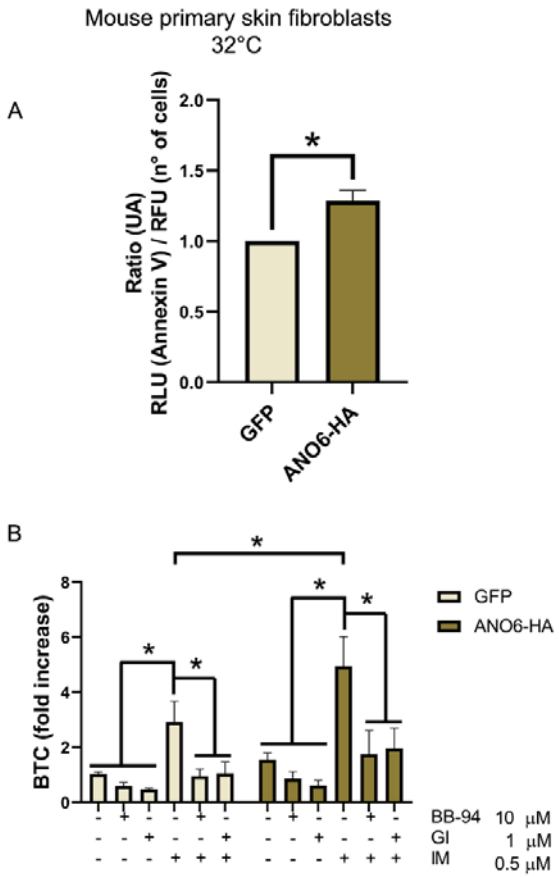

Supplementary Figure 2: Overexpression of ANO6-HA enhances IM-induced ADAM10 shedding activity in mouse primary skin fibroblasts incubated at 32°C and hypoxic conditions

(A) PS in the outer leaflet of the cell membrane was evaluated through the ratio between the Annexin V (RLU) and n° of cells (RFU) in cells transfected with ANO6-HA or GFP as a control, in MPSF incubated at 32°C under hypoxic conditions. Results are mean ± SEM; n=3. For statistical analysis, mean values were compared using an unpaired t test; *p ≤ 0.05. (B) MPSF were transfected with the AP-tagged ADAM10 substrate BTC or GFP. BTC shedding was evaluated by treating cells for 30 min with a general inhibitor of metalloproteases (Batimastat, BB, 10 µM) or an ADAM10 inhibitor (GI254023X, GI, 1 µM), and then cells were stimulated for 1 h with ionomycin (IM, 0.5 µM). Vehicle: DMSO. Results are mean ± SEM; n=4. For statistical analysis, mean values were compared using an ANOVA and Tukey's post-hoc test; *p ≤ 0.05.

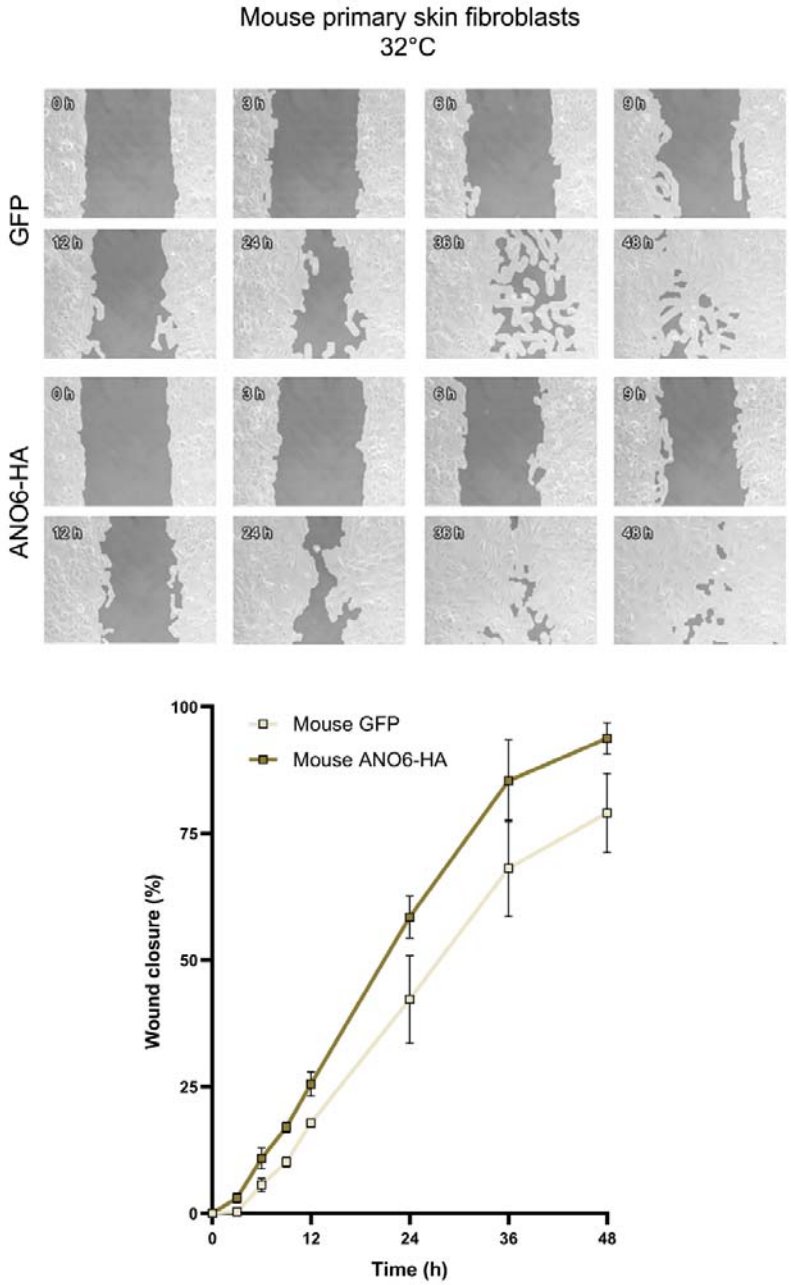

Supplementary Figure 3: Overexpression of ANO6-HA enhances migration in mouse primary skin fibroblasts incubated at 32°C and hypoxic conditions

MPSF were transfected with ANO6-HA or GFP. Images were taken at 0, 3, 6, 9,12, 24, 36, and 48 h after removed the silicone insert for gap creation. Quantification of the wound closure over the time is showed. Results are mean ± SEM; n=2.

Discussion

NMRs display very low incidence of cancer and yet mechanisms underpinning this are still not fully understood (Buffenstein et al., 2022; Hadi et al., 2021). Demonstration that NMR cells are susceptible to oncogenic transformation (Hadi et al., 2020) suggests that other mechanisms likely explain why oncogenic events rarely result in cancer, for example a low somatic mutation rate (Cagan et al., 2022) or altered immune response (Oka et al., 2022). A key part of cancer development is the ability of cells to proliferate and migrate, which involves navigating the extracellular matrix. CD44 is a receptor for several extracellular matrix components (Banerji et al., 2007; Chen et al., 2020; Radotra et al., 1994), and is considered a marker of cancer (Corte et al., 2010; Hassn Mesrati et al., 2021; Leung et al., 2010; Lokeshwar et al., 1995; Olsson et al., 2011; Takaishi et al., 2009; Zoller, 2011). CD44 can be cleaved in the ectodomain by metalloproteases (Nagano et al., 2004; Nagano and Saya, 2004; Nakamura et al., 2004), resulting in a sequential proteolytic cleavage of the intracellular domain by γ-secretase, generating release of the CD44 intracellular domain fragment (CD44ICD) (Murakami et al., 2003), which translocates to the nucleus, regulating transcriptional activity through transcription factors as CBP/p300 and STAT3 (Okamoto et al., 2001). In addition, CD44ICD regulates the transcription of proteins like MMP-9 (Miletti-Gonzalez et al., 2012), IFN-γ (Schultz et al., 2018) and CD44 itself (Okamoto et al., 2001).

Patients with cancer have higher levels of CD44 cleavage (Okamoto et al., 2002; Yamane et al., 1999). ADAM10 is one of the metalloproteases that cleaves extracellular CD44 (Anderegg et al., 2009; Murai et al., 2006; Nagano et al., 2004; Pan et al., 2012) and is involved in the chemo-resistance of breast cancer cells (Cheng et al., 2021). Interestingly, our data shows that IM, which is well characterised as being able to induce ADAM10 shedding activity (Maretzky et al., 2005; Reiss and Bhakdi, 2012), only does so in the oncogenic NMR SV40-Ras skin fibroblasts, but not in NPSF. Comparing MPSF and NPSF, we observed that IM only induces ADAM10-dependent CD44 cleavage in mouse cells, suggesting that the absence of CD44 cleavage in the NPSF could be a mechanism by which the NMR cells are resistant to developing cancer. Previous studies have suggested that early contact inhibition is a mechanism that contributes to cancer resistance of NMR by arresting the cell cycle (Seluanov et al., 2009). Furthermore, a CD44-blocking antibody was used to demonstrate that CD44 is important for early contact inhibition (Tian et al., 2013). Therefore, our data provide further evidence for an important role of CD44 in contributing to cancer resistance in NMRs.

ADAM10 is of particular interest in cancer, being highly expressed, up-regulated and involved in patients with glioblastoma (Siney et al., 2017), gastric cancer (Wang et al., 2019a), lung cancer (Guo et al., 2012), and pancreatic cancer (Gaida et al., 2010) to name but a few. It has also been shown that overexpression of ADAM10 is associated with a worse prognosis for pancreatic and lung cancers (Trerotola et al., 2021). We therefore evaluated the expression and the shedding activity of ADAM10 to understand if the absence of IM-induced CD44 cleavage observed in NPSF was simply due to lack of ADAM10 expression. Interestingly, comparing ADAM10 protein expression in MPSF and NPSF, higher levels of the pro form were found in NMR cells, and no difference was detected in expression of mature ADAM10 across species. The cleavage site of ADAM substrates is located very close to the cell surface (Horiuchi, 2013), and we found that IM induced ADAM10 translocation in both MPSF and NPSF, as well as in the oncogenic mouse and NMR SV40-Ras skin fibroblasts. Thus, a lack of IM-induced ADAM10-dependent CD44

cleavage is not due to an absence of ADAM10 expression or aberrant plasma membrane translocation. Using cell-based assays to measure ADAM10-dependent BTC shedding, we found that IM induces BTC shedding in MPSF, mouse SV40-Ras skin fibroblasts, and in NMR SV40-Ras skin fibroblasts, but not in the NPSF, results consistent with the absence of IM-induced CD44 cleavage in NPSF, thus suggesting that the regulation of ADAM10 shedding activity could be a key factor in NMR cancer resistance because without efficient CD44 cleavage cell migration is impaired and thus making oncogenic cells vulnerable to degradation.

It is well understood that the cell membrane lipid composition regulates the shedding activity of ADAM10. For example, low cholesterol levels in the cell membrane increase ADAM10 shedding activity, whereas cholesterol enrichment does not (Matthews et al., 2003). Interestingly, the NMR brain has higher levels of cholesterol compared to the mouse brain (Frankel et al., 2020), which may thus help to explain why under basal conditions there is an absence of IM-induced ADAM10-dependent CD44 cleavage in NPSF. Moreover, PS exposure in the outer leaflet of the cell membrane also regulates ADAM10 shedding activity. The cationic amino acid residues present in the stalk region of ADAM10 are proposed to interact with the negatively charged PS head group located in the outer leaflet of the cell membrane triggering the ADAM10 sheddase function (Bleibaum et al., 2019). Using mass spectrometry, no difference in the concentration of PS from NMR and mouse total brain lipid extract was detected (Frankel et al., 2020). However, here we found approximately 3-fold higher levels of PS exposure on the cell surface of oncogenic NMR SV40-Ras skin fibroblasts compared to NPSF, and no changes in the PS externalization in mouse SV40-Ras compared with the MPSF. Taking this into consideration, the higher exposure of PS in the NMR SV40-Ras fibroblasts could explain why IM induces approximately 3-fold higher BTC shedding in the NMR vs. mouse SV40-Ras skin fibroblasts. By comparison, PS exposure on the outer leaflet of the cell membrane in NPSF is only about 10% compared to the level in MPSF. This lower level of PS externalization found in NPSF could explain the absence of IM-induced CD44 cleavage and ADAM10 shedding activity in NPSF. Consistent with this, when we overexpressed a hyperactive form of ANO6, a scramblase that regulates the PS exposure in the outer leaflet of the cell membrane (Bleibaum et al., 2019), we observed an increase in the PS exposure in NPSF, and as expected, IM-induced ADAM10 shedding activity was “rescued” in these cells as evaluated by the shedding of BTC.

It has been shown that CD44 cleavage promotes tumour cell migration (Kawano et al., 2000; Kolliopoulos et al., 2021; Kung et al., 2012; Sugahara et al., 2003) and that ADAM10-dependent CD44 cleavage promotes migration of pituitary adenoma cell (Pan et al., 2012), of glioblastoma (Murai et al., 2004), and melanoma cells (Anderegg et al., 2009). In line with these findings, we observed that the percentage of wound closure in NPSF was lower than that of MPSF, but that higher closure occurred following overexpression of ANO6-HA, thus suggesting that CD44 cleavage and ADAM10 shedding activity might contribute to NMR cancer resistance.

Taking all this data together, our findings suggest that the lower level of PS in the outer membrane of NPSF prevents the shedding activity of ADAM10 in response to IM and thus regulation of ADAM10 shedding activity by PS localization in the inner and outer leaflet of the cell membrane might be an important mechanism underlying cancer resistance in NMRs. Future work will be focused on understanding the regulation of PS localization in NPSF,

including the roles of scramblases and flippases, as well as studying the regulation and localization of Ca^{2+} in the NMR cells compared to those of mice.

Author contributions

P.U-M and E.StJ.S conceived the experiments, P.U-M carried out experiments, L.A.P took confocal images, P.U-M and E.StJ.S analysed data, P.U-M and E.StJ.S wrote the manuscript. All authors provided input to and approved the final manuscript.

Acknowledgments

This work was funded by the Dunhill Medical Trust (RPGF2002\188). The plasmid for alkaline phosphatase (AP)-tagged BTC expression was a kind gift from Dr Carl P. Blobel (Hospital for Special Surgery, New York, USA). The plasmid for the hyperactive form of ANO6 (ANO6-HA) was a kind gift from Dr Karina Reiß (Department of Dermatology, University of Kiel, 24105 Kiel, Germany).

Declaration of interests

These authors declare no conflicts of interest.

STAR Methods

RESOURCE AVAILABILITY

Lead Contact

Further information and requests for resources and reagents should be directed to and will be fulfilled by the lead contact, Dr Ewan St. John. Smith (es336@cam.ac.uk).

Materials availability

This study did not generate new unique reagents.

Data and code availability

All data reported in this paper will be shared by the lead contact upon request.

This paper does not report original code.

Any additional information required to reanalyze the data reported in this paper is available from the lead contact upon request.

EXPERIMENTAL MODEL AND SUBJECT DETAILS

Experiments were performed on cells extracted from a mixture of male and female C57BL6/J mice (8-15 weeks old), and a mixture of male and female, non-breeder NMRs (7-43 month old). Mice were conventionally housed with nesting material and a red plastic shelter in temperature-controlled rooms at 21° C, with a 12 h light/dark cycle and access to food and water ad libitum. Naked mole-rats were bred in-house and maintained in an inter-connected network of cages in a humidified (~55 %) temperature-controlled room at 28° C, with red lighting (08:00-16:00) and had access to food ad libitum. In addition, a heat cable provided extra warmth under 2-3 cages/colony. Mice were humanely killed by cervical dislocation of the neck and cessation of circulation, whereas naked mole-rats were killed by CO2 exposure followed by decapitation. Experiments were conducted under the Animals (Scientific Procedures) Act 1986 Amendment Regulations 2012 under a Project License (P7EBFC1B1) granted to E. St. J. Smith by the Home Office and approved by the University of Cambridge Animal Welfare Ethical Review Body.

NMR primary skin fibroblasts were cultured in DMEM high glucose (Gibco #41965-039) supplemented with 15% fetal bovine serum (Sigma-Aldrich #F7524-500ML), 1X non-essential amino acids (Gibco #1140-050), 1 mM sodium pyruvate (Gibco #11360-039), 100 units ml^{-1} penicillin, 100 µg ml^{-1} streptomycin (Gibco #15140122) and 100 µg ml^{-1} Primocin (InvivoGen #ant-pm-2). Cells were incubated in a humidified 32 °C incubator with 5% CO_2 and 3% O_2.

NMR SV40-Ras skin fibroblasts skin fibroblasts were cultured in DMEM high glucose (Gibco # 41965-039) supplemented with 15% fetal bovine serum (Sigma-Aldrich #F7524-500ML), 1X non-essential amino acids (Gibco #1140-050), 1 mM sodium pyruvate (Gibco #11360-039) and 100 units ml^{-1} penicillin, 100 µg ml^{-1} streptomycin (Gibco #15140122). Cells were incubated in a humidified 32 °C incubator with 5% CO_2 and 3% O_2.

Mouse primary skin fibroblasts were cultured in DMEM high glucose (Gibco # 41965-039) supplemented with 15% fetal bovine serum (Sigma-Aldrich #F7524-500ML), 100 units ml^{-1} penicillin, 100 µg ml^{-1} streptomycin (Gibco #15140122) and 100 µg ml^{-1} Primocin (InvivoGen #ant-pm-2). Cells were incubated in a humidified 37 °C incubator with 5% CO_2.

Mouse SV40-Ras skin fibroblasts were cultured in DMEM high glucose (Gibco # 41965-039) supplemented with 15% fetal bovine serum (Sigma-Aldrich #F7524-500ML) and 100 units ml^{-1} penicillin, 100 µg ml^{-1} streptomycin (Gibco #15140122). Cells were incubated in a humidified 37 °C incubator with 5% CO_2.

METHOD DETAILS

NMR primary skin isolation

Following CO_2 exposure and decapitation, skin tissue was collected from each animal on ice-cold PBS 1X (Gibco #70011-044). Skin came from the underarm, dorsal and ventral surfaces of each animal, and was cleaned of any fat or muscle tissue and generously sprayed with 70% ethanol. Once cleaned, the tissue was washed twice with PBS 1X before

finely mincing with sterile blades (Swann Morton #BS2982). Minced skin was then mixed with 5 ml of NMR Cell Isolation Medium containing 10 mg ml^{-1} collagenase (Sigma-Aldrich #C9891), 1000 units ml^{-1} hyaluronidase (Sigma-Aldrich #H3506) in DMEM high glucose (Gibco #41965-039) and incubated at 37°C for 3 – 5 hours. The tissue was briefly vortexed every 30 minutes to aid cell dissociation and inspected for cell dissociation. After complete dissociation, cells were pelleted by centrifuging at 500 g for 3 minutes and resuspended in PBS, then the cells were centrifuged again at 500 g for 3 minutes and resuspended in NMR cell culture medium (DMEM high glucose (Gibco #41965-039) supplemented with 15% fetal bovine serum (Sigma-Aldrich #F7524-500ML), 1X non-essential amino acids (Gibco #11140-050), 1 mM sodium pyruvate (Gibco #11360-039), 100 units ml^{-1} penicillin, 100 µg ml^{-1} streptomycin (Gibco #15140122) and 100 µg ml^{-1} Primocin (InvivoGen #ant-pm-2)). This cell suspension was passed through 70 µm filter (Falcon #352350) and seeded on treated cell culture flask (T-75 Greiner Bio-One #658175). The cells were incubated in a humidified 32 °C incubator with 5% CO_2 and 3% O_2.

Mouse primary skin isolation

Following CO_2 exposure and cervical dislocation, both mice ears were collected from each animal on ice-cold PBS 1X (Gibco # 70011-044). Skin was cleaned of any hair and generously sprayed with 70% ethanol. Once cleaned, the tissue was washed twice with PBS 1X before finely mincing with sterile blades (Swann Morton #BS2982). Minced skin was then mixed with 5 ml of 10 mg ml^{-1} collagenase (Sigma-Aldrich #C9891), 1000 units ml^{-1} hyaluronidase (Sigma-Aldrich #H3506) in DMEM high glucose (Gibco #41965-039) and incubated at 37°C for 3 – 5 hours. The tissue was briefly vortexed every 30 minutes to aid cell dissociation and inspected for cell dissociation. After complete dissociation, cells were pelleted by centrifuging at 500 g for 3 minutes and resuspended in PBS 1X, then the cells were centrifuged again at 500 g for 3 minutes and resuspended in mouse cell culture medium (DMEM high glucose (Gibco # 41965-039) supplemented with 15% fetal bovine serum (Sigma-Aldrich #F7524-500ML), 100 units ml^{-1} penicillin, 100 µg ml^{-1} streptomycin (Gibco #15140122) and 100 µg ml^{-1} Primocin (InvivoGen # ant-pm-2)). This cell suspension was passed through 70 µm filter (Falcon # 352350) and seeded on treated cell culture Flask (T-75 Greiner Bio-One # 658175). The cells were incubated in a humidified 37 °C incubator with 5% CO_2.

Protein Extraction and Western Blotting

Protein extraction was performed by homogenizing cells in a buffer containing 150 mM NaCl, 10 mg ml^{-1} PMSF, 60 mM DTT, 1% NP-40, 1 mM sodium orthovanadate and 50 mM Tris–HCl pH 7.4, plus a general metalloprotease inhibitor BB-94 10 µM (Calbiochem #196440) and protease inhibitor cocktail (Sigma-Aldrich #P2714) including 2 mM AEBSF [4-(2-Aminoethyl) benzenesulfonylfluoride hydrochloride], 0.3 µM aprotinin, 130 µM bestatin hydrochloride, 14 µME-64, 1 mM EDTA, 1 µM leupeptin hemisulfatein, and then centrifuging for 10 min at 13,200 x rpm at 4°C. The samples were run on a 15% polyacrylamide gel (SDS–PAGE) under reducing and denaturing conditions, and then transferred to nitrocellulose membrane (Thermo Fisher #88018). Nitrocellulose membrane was blocked with 3% (w/v) non-fat milk (Sigma-Aldrich #70166), 0.1% Tween-20 in TBS, pH 7.4. Then the membrane was incubated overnight at 4˚C with one of the following antibodies: anti-CD44

(0.04 µg ml^{-1}, abcam #ab157107), anti-ADAM10 (0.04 µg ml^{-1}, Invitrogen #PA5-87899), anti-ANO6 (0.5 µg ml^{-1}, Invitrogen #PA5-35240) or anti-β-actin (8H10D10) (1:10,000, Cell Signaling cat#3700S) as a loading control. Membranes were then incubated with a donkey anti-rabbit IgG secondary antibody conjugated with IRDye® 800CW (0.2 µg ml^{-1}, LI-COR #926-32213) and donkey anti-mouse IgG secondary antibody conjugated with IRDye® 680RD (0.2 µg ml^{-1}, LI-COR #926-68072) in blocking solution for 1 h at room temperature. Protein bands were evaluated using the Oddysey®XF Imaging System (LI-COR) and images were analyzed using the Image Studio Lite software (LI-COR).

Membrane protein biotinylation

Fibroblasts were growth in a 10 cm dish (Cyto-one #CC7682-3394). Mouse and NMR primary skin fibroblasts were treated for 1 h with IM 0.5 µM or DMSO as vehicle in DMEM high glucose (Gibco # 41965-039). Mouse and NMR SV40-Ras skin fibroblasts were treated for 10 min with IM 2.5 µM or DMSO as vehicle in DMEM high glucose (Gibco # 41965-039). After the treatment, the culture medium was eliminated and then the cells were washed two times with Hanks-Ca^{2+} medium pH 7,4. Then, the cells were incubated with EZ-Link™ Sulfo-NHS-SS-Biotin (0.5 mg ml^{-1}, Thermo Fisher #21331) for 30 min at 4°C. The biotin was washed three times with Hanks-Ca^{2+} supplemented with 1 mg ml^{-1} glycine. After that, the cells were recollected in a solution of distillated water with protease inhibitors cocktail (Sigma-Aldrich #P2714) and centrifuged at 13,200 x rpm for 2 min at 4°C. The pellet was resuspended in a buffer containing 150 mM NaCl, 10 mg/ml PMSF, 60 mM DTT, 1% NP-40, 1 mM sodium orthovanadate and 50 mM Tris–HCl pH 7.4, plus a general metalloprotease inhibitor BB-94 10 µM (Calbiochem #196440) and protease inhibitor cocktail (Sigma-Aldrich #P2714) including 2 mM AEBSF [4-(2-Aminoethyl) benzenesulfonylfluoride hydrochloride], 0.3 µM aprotinin, 130 µM bestatin hydrochloride, 14 µME-64, 1 mM EDTA, 1 µM leupeptin hemisulfatein. Then the protein concentration (total fraction) was calculated. 200 µg of protein was precipitated with NeutrAvidin™ Agarose Resins (Thermo Fisher Scientific #29201) after an incubation of 1 h at 4°C with occasional manual agitation. The pellet was washed with Hanks- supplemented with 0.1% SDS and 1% NP-40 and then centrifuged at 13,200 x rpm for 2 min at 4°C and resuspended with 20 µl Hanks-Ca^{2+} supplemented with 1 mg ml^{-1} glycine, pH 2,8. Then the sample was centrifuged in the same conditions above and the supernatant was rescued (this was the biotinylated fraction). All fraction were running in a 10% polyacrylamide gel (SDS–PAGE) under reducing and denaturing conditions.

Immunofluorescence

Mouse and NMR primary skin fibroblasts were grown in a MatTek (MatTek life sciences P35GC-1.5-14-C) dish under the conditions explained above. The localization of ADAM10 was assayed in the fibroblasts treated for 1 h with IM 0.5 µM or DMSO as vehicle. After the treatment fibroblasts were fixed in 100% methanol for 15 min at -20°C and then permeabilized with 0.1% Triton X-100. To prevent unspecific binding the samples were treated with 3% BSA (Sigma-Aldrich #A2153) in TBS containing 0.1% Tween-20 for 1 h at room temperature. A primary antibody against ADAM10 (Invitrogen #PA5-87899) was applied at 1 µg ml^{-1} diluted in 3% BSA-TBS containing 0.1% Tween-20 to the dish, which were incubated overnight at 4°C in a humidified chamber, after that the dish had been

washed three times for 10 min in TBS containing 0.1% Tween-20. Then Goat anti-Rabbit IgG (H+L) Cross-Adsorbed Secondary Antibody, Alexa Fluor™ 488 (Invitrogen #A-11008) at 1 µg ml^{-1} diluted in 3% BSA-TBS containing 0.1% Tween-20 was added to the dish and then incubated for 1 h at room temperature, after that the dishes were washed three times for 10 min in TBS containing 0.1% Tween-20. Then, 5 µg ml^{-1} of wheat germ agglutinin was added and incubated for 10 min at 37°C. After that the dishes were washed as before. Then, NucRed™ Live 647 (Invitrogen #R37106) was added to the dish and incubated for 5 min at room temperature. Finally, the dishes were washed as above. The cells were observed using a Leica SP5 laser-scanning confocal microscope with 63x oil objective. Images were acquired in sequential scan mode: wheat germ agglutinin fluorescence was excited with a 405 nm laser and emission 415 - 475 nm recorded, Alexa Fluor™ 488 was excited with a 488 nm laser and emission between 498 - 590 nm captured, a 633 nm laser was used to excite NucRed™ Live 647 and emission between 645 - 633 nm detected. Composite images were created in Image J.

Cell transfection

Mouse and NMR primary and SV40-Ras skin fibroblasts were transfected with the plasmid (AP)-tagged BTC (Horiuchi et al., 2007) kindly donated by Dr. Carl Blobel (Hospital for Special Surgery, New York, USA) or with the hyperactive ANO6 (ANO6-HA) (Bleibaum et al., 2019) kindly donated by Dr Karina Reiß (Department of Dermatology, University of Kiel, 24105 Kiel, Germany). Briefly, fibroblasts were seeded to 80% confluence and the following day fibroblasts were washed with PBS 1X and cultured in DMEM high glucose (Gibco # 41965-039) at the same conditions mentioned above. After that, the cells were cultured for 24 h with a complex DNA- FuGENE® HD Transfection Reagent (Promega #E2311) in a ratio 1:3 prepared in Opti-MEM reduced serum medium (Gibco #31985070).

ADAM10 shedding assay

For the shedding assay, fibroblasts were seeded in 12 well plates (Corninig Costar #3513). Every condition of the experiment was performed in non-transfected and transfected cells with the (AP)-tagged BTC plasmid. After 24 h, cells were washed once in PBS 1X and incubated for 30 min in Opti-MEM reduced serum medium (Gibco # 31985070). Then, treatment with IM and inhibitors (general inhibitor of metalloproteases (Batimastat, BB, 10 µM), an ADAM10 inhibitor (GI254023X, GI, 1 µM) or an ADAM10/ADAM17 inhibitor (GW280264X, GW, 1 µM)) were performed as indicated in the results section. After the treatment, conditioned media were collected and cells were lysed with a solution containing 2.5% Triton X-100 (Sigma-Aldrich #T8787), 1 mM 1-10 phenanthroline (Sigma-Aldrich #131377) and 1 mM EDTA (Fisher Scientific #10618973). 100 µl of conditional media and 10 µl of cell lysate were added into 96 well plates (Starlab #E2996-1610). Then 90 µl of AP-buffer (100 mM Tris, 100 mM NaCl, 20 mM MgCl2, pH 9.5) was added only to the cell lysate wells. After that, both conditional media and cell lysate, were incubated with 100 µl of 2 mg ml^{-1} p-NPP (p-nitrophenyl phosphate) substrate (Thermo Fisher #34045) diluted in AP-buffer. Then the plate was incubated for 1 h at 37°C. The AP activity was measured by a spectrophotometer (CLARIOstar, BMG Labtech) at 405 nm. Three identical wells were prepared, and the ratio of AP activity in the medium and that of the cell lysate plus medium

was calculated. For stimulated shedding or vehicle, the fold increase in the ratio of AP activity obtained after stimulation is shown relative to ratio of AP activity in control wells. Each experiment was conducted at least three times. Transfection efficiency was controlled by determining the ratio of the activity of AP in the medium over the AP-activity in the cells plus the medium.

PS in the outer leaflet of the cell membrane

20,000 fibroblasts per well were seeded in a white 96 well plate (CytoOne #CC7682-7596). The following day, cells were washed with PBS 1X and incubated with Imaging media (140 mM NaCl, 2.5 mM KCl, 1.8 mM $CaCl_2$, 1 mM $MgCl_2$, 20 mM HEPES) supplemented with 15% of fetal bovine serum (Sigma-Aldrich #F7524-500ML). PS exposure was evaluated through the ratio between the Annexin V and n° of cells. Annexin V binding to PS was measured using the RealTime-Glo™ Annexin V luminescence assay (Promega #JA1000), following the instruction of the kit. Briefly, Annexin V NanoBiT™ Substrate, Annexin V-SmBiT and Annexin V-LgBiT were added to the cells and incubated for 30 min at 37°C. As product of the binding of PS to annexin V a luminescence signal is detected. RLU was measured using a luminescence microplate reader (CLARIOstar, BMG Labtech). To determinate the number of cells, after measurement of the RFU, cells were washed once with PBS 1X and then incubated with NucRed™ Live 647 ReadyProbes® reagent (Invitrogen #R37106) in Imaging media for 15 min at room temperature. After that the cells were washed with PBS 1X and the RFU was measured using a fluorescence microplate reader (CLARIOstar, BMG Labtech). Three identical wells were prepared, and the ratio of RLU/RFU was calculated.

Wound closure assay

20,000 fibroblasts in each well of a culture-insert 2 well in µ-dish 35 mm, high (Ibidi #81176) and transfected as mentioned above. The following day, the silicon insert was removed from the dish and cells were washed once with PBS 1X and DMEM high glucose media (Gibco #41965-039) supplemented with 5% of fetal bovine serum (Sigma-Aldrich #F7524-500ML) was added. During all the experiment fibroblasts were culture in the conditions mentioned above. To measure the wound closure percentage, 4 pictures from each dish were taken at 0, 3, 6, 9, 12, 24, 36 and 48 h using a 5MP USB 2.0 Color CMOS C-Mount Microscope Camera (AmScope, MU500-CK-3PL). Wound closure area was calculated using the TScratch software (Geback et al., 2009).

Key resources table

REAGENT or RESOURCE	SOURCE	IDENTIFIER
Antibodies		
Rabbit polyclonal anti-CD44	abcam	#ab157107
Rabbit polyclonal anti-ADAM10	Invitrogen	#PA5-87899
Rabbit polyclonal anti-ANO6	Invitrogen	#PA5-35240
Mouse monoclonal anti-β-actin (8H10D10)	Cell Signaling	#3700S
IRDye® 800CW Donkey anti-Rabbit IgG	LI-COR	#926-32213

IRDye® 680RD Donkey anti-Mouse IgG	LI-COR	#926-68072
Goat anti-Rabbit IgG (H+L) Cross-Adsorbed Secondary Antibody, Alexa Fluor™ 488	Invitrogen	#A-11008
Bacterial and virus strains		
E. Coli (DH5a) for plasmid maintenance	Invitrogen	#18265017
Chemicals, peptides, and recombinant proteins		
Fetal bovine serum	Sigma-Aldrich	#F7524-500ML
DMEM high glucose	Gibco	#41965-039
Opti-MEM reduced serum medium	Gibco	#31985070
Non-essential amino acids	Gibco	#1140-050
Sodium pyruvate	Gibco	#11360-039
Penicillin and Streptomycin	Gibco	#15140122
Primocin	InvivoGen	#ant-pm-2
PBS 10X	Gibco	#70011-044
Ethanol	Sigma-Aldrich	#32221
Methanol	Sigma-Aldrich	#32213
Collagenase from Clostridium histolyticum	Sigma-Aldrich	#C9891
Hyaluronidase from bovine testes	Sigma-Aldrich	#H3506
NaCl	Fisher Scientific	#10092740
KCl	Fisher Scientific	#10375810
$CaCl_2$ - 2 H_2O	Fisher Scientific	# 10171800
HEPES	Gibco	#15630-056
EDTA	Fisher Scientific	#10618973
Tris Base	Fisher Scientific	#10376743
$MgCl_2$ – 6 H_2O	Fisher Scientific	#10647032
PMSF	Thermo Fisher	#36978
NP-40	Sigma-Aldrich	#74385
Sodium Orthovanadate	Sigma-Aldrich	#S6508
Triton X-100	Sigma-Aldrich	#T8787
BB-94	Calbiochem	#196440
Protease inhibitor cocktail	Sigma-Aldrich	#P2714
30% acrylamide and bis-acrylamide solution, 29:1	Bio-Rad	#161-0156
SDS	Fisher Scientific	#10607633
Nitrocellulose membrane	Thermo Fisher	#88018
non-fat milk	Sigma-Aldrich	#70166
Tween 20	Sigma-Aldrich	#P1379
EZ-Link™ Sulfo-NHS-SS-Biotin	Thermo Fisher	#21331
Glycine	Sigma-Aldrich	#G7126
NeutrAvidin™ Agarose Resins	Thermo Fisher	#29201
Ionomycin	Cambridge Bioscience	#CAY11932
DMSO	Sigma-Aldrich	#D8418
BSA	Sigma-Aldrich	#A2153
Wheat Germ Agglutinin	Biotium	#29028
FuGENE® HD Transfection Reagent	Promega	#E2311
GI254023X	Generon	#HY-19956
GW280264X	Generon	# HY-115670
1-10 phenanthroline	Sigma-Aldrich	#131377
p-NPP substrate	Thermo Fisher	#34045
NucRed™ Live 647 ReadyProbes	Invitrogen	#R37106
Critical commercial assays		
RealTime-Glo™ Annexin V assay	Promega	#JA1000

Experimental models: Cell lines		
NMR SV40-Ras skin fibroblasts	Hadi et al., 2020	N/A
Mouse SV40-Ras skin fibroblasts	Hadi et al., 2020	N/A
Recombinant DNA		
AP-BTC	Horiuchi et al., 2007	N/A
ANO6-HA	Bleibaum et al., 2019	N/A
pGFP	Clontech	#632370
Software and algorithms		
Image Studio Lite software	LI-COR	https://www.licor.com/bio/image-studio-lite/
Fiji	ImageJ2	https://imagej.net/software/fiji/
TScratch	Geback et al., 2009	https://github.com/cselab/TScratch/blob/master/INSTALL

Bibliography

Anderegg, U., Eichenberg, T., Parthaune, T., Haiduk, C., Saalbach, A., Milkova, L., Ludwig, A., Grosche, J., Averbeck, M., Gebhardt, C.*, et al.* (2009). ADAM10 is the constitutive functional sheddase of CD44 in human melanoma cells. J Invest Dermatol *129*, 1471-1482.
Banerji, S., Wright, A.J., Noble, M., Mahoney, D.J., Campbell, I.D., Day, A.J., and Jackson, D.G. (2007). Structures of the Cd44-hyaluronan complex provide insight into a fundamental carbohydrate-protein interaction. Nat Struct Mol Biol *14*, 234-239.
Bleibaum, F., Sommer, A., Veit, M., Rabe, B., Andra, J., Kunzelmann, K., Nehls, C., Correa, W., Gutsmann, T., Grotzinger, J.*, et al.* (2019). ADAM10 sheddase activation is controlled by cell membrane asymmetry. J Mol Cell Biol *11*, 979-993.
Bourguignon, L.Y. (2008). Hyaluronan-mediated CD44 activation of RhoGTPase signaling and cytoskeleton function promotes tumor progression. Semin Cancer Biol *18*, 251-259.
Bourguignon, L.Y., Peyrollier, K., Gilad, E., and Brightman, A. (2007). Hyaluronan-CD44 interaction with neural Wiskott-Aldrich syndrome protein (N-WASP) promotes actin polymerization and ErbB2 activation leading to beta-catenin nuclear translocation, transcriptional up-regulation, and cell migration in ovarian tumor cells. J Biol Chem *282*, 1265-1280.
Buffenstein, R. (2005). The naked mole-rat: a new long-living model for human aging research. J Gerontol A Biol Sci Med Sci *60*, 1369-1377.
Buffenstein, R., Amoroso, V., Andziak, B., Avdieiev, S., Azpurua, J., Barker, A.J., Bennett, N.C., Brieno-Enriquez, M.A., Bronner, G.N., Coen, C.*, et al.* (2022). The naked truth: a comprehensive clarification and classification of current 'myths' in naked mole-rat biology. Biol Rev Camb Philos Soc *97*, 115-140.
Cagan, A., Baez-Ortega, A., Brzozowska, N., Abascal, F., Coorens, T.H.H., Sanders, M.A., Lawson, A.R.J., Harvey, L.M.R., Bhosle, S., Jones, D.*, et al.* (2022). Somatic mutation rates scale with lifespan across mammals. Nature *604*, 517-524.
Chen, K.L., Li, D., Lu, T.X., and Chang, S.W. (2020). Structural Characterization of the CD44 Stem Region for Standard and Cancer-Associated Isoforms. Int J Mol Sci *21*.
Cheng, Y., Lin, L., Li, X., Lu, A., Hou, C., Wu, Q., Hu, X., Zhou, Z., Chen, Z., and Tang, F. (2021). ADAM10 is involved in the oncogenic process and chemo-resistance of triple-negative breast cancer via regulating Notch1 signaling pathway, CD44 and PrPc. Cancer Cell Int *21*, 32.
Corte, M.D., Gonzalez, L.O., Junquera, S., Bongera, M., Allende, M.T., and Vizoso, F.J. (2010). Analysis of the expression of hyaluronan in intraductal and invasive carcinomas of the breast. J Cancer Res Clin Oncol *136*, 745-750.
Edrey, Y.H., Hanes, M., Pinto, M., Mele, J., and Buffenstein, R. (2011). Successful aging and sustained good health in the naked mole rat: a long-lived mammalian model for biogerontology and biomedical research. ILAR J *52*, 41-53.
Frankel, D., Davies, M., Bhushan, B., Kulaberoglu, Y., Urriola-Munoz, P., Bertrand-Michel, J., Pergande, M.R., Smith, A.A., Preet, S., Park, T.J.*, et al.* (2020). Cholesterol-rich naked mole-rat brain lipid membranes are susceptible to amyloid beta-induced damage in vitro. Aging (Albany NY) *12*, 22266-22290.
Gaida, M.M., Haag, N., Gunther, F., Tschaharganeh, D.F., Schirmacher, P., Friess, H., Giese, N.A., Schmidt, J., and Wente, M.N. (2010). Expression of A disintegrin and metalloprotease 10 in pancreatic carcinoma. Int J Mol Med *26*, 281-288.
Geback, T., Schulz, M.M., Koumoutsakos, P., and Detmar, M. (2009). TScratch: a novel and simple software tool for automated analysis of monolayer wound healing assays. Biotechniques *46*, 265-274.
Guo, J., He, L., Yuan, P., Wang, P., Lu, Y., Tong, F., Wang, Y., Yin, Y., Tian, J., and Sun, J. (2012). ADAM10 overexpression in human non-small cell lung cancer correlates with cell migration and invasion through the activation of the Notch1 signaling pathway. Oncol Rep *28*, 1709-1718.

Guo, Y.J., Liu, G., Wang, X., Jin, D., Wu, M., Ma, J., and Sy, M.S. (1994). Potential use of soluble CD44 in serum as indicator of tumor burden and metastasis in patients with gastric or colon cancer. Cancer Res *54*, 422-426.
Hadi, F., Kulaberoglu, Y., Lazarus, K.A., Bach, K., Ugur, R., Beattie, P., Smith, E.S.J., and Khaled, W.T. (2020). Transformation of naked mole-rat cells. Nature *583*, E1-E7.
Hadi, F., Smith, E.S.J., and Khaled, W.T. (2021). Naked Mole-Rats: Resistant to Developing Cancer or Good at Avoiding It? Adv Exp Med Biol *1319*, 341-352.
Hartmann, D., de Strooper, B., Serneels, L., Craessaerts, K., Herreman, A., Annaert, W., Umans, L., Lubke, T., Lena Illert, A., von Figura, K.*, et al.* (2002). The disintegrin/metalloprotease ADAM 10 is essential for Notch signalling but not for alpha-secretase activity in fibroblasts. Hum Mol Genet *11*, 2615-2624.
Hassn Mesrati, M., Syafruddin, S.E., Mohtar, M.A., and Syahir, A. (2021). CD44: A Multifunctional Mediator of Cancer Progression. Biomolecules *11*.
Holmes, M.M., and Goldman, B.D. (2021). Social Behavior in Naked Mole-Rats: Individual Differences in Phenotype and Proximate Mechanisms of Mammalian Eusociality. Adv Exp Med Biol *1319*, 35-58.
Horiuchi, K. (2013). A brief history of tumor necrosis factor alpha--converting enzyme: an overview of ectodomain shedding. Keio J Med *62*, 29-36.
Horiuchi, K., Le Gall, S., Schulte, M., Yamaguchi, T., Reiss, K., Murphy, G., Toyama, Y., Hartmann, D., Saftig, P., and Blobel, C.P. (2007). Substrate selectivity of epidermal growth factor-receptor ligand sheddases and their regulation by phorbol esters and calcium influx. Mol Biol Cell *18*, 176-188.
Ishii, S., Ford, R., Thomas, P., Nachman, A., Steele, G., Jr., and Jessup, J.M. (1993). CD44 participates in the adhesion of human colorectal carcinoma cells to laminin and type IV collagen. Surg Oncol *2*, 255-264.
Jalkanen, S., and Jalkanen, M. (1992). Lymphocyte CD44 binds the COOH-terminal heparin-binding domain of fibronectin. J Cell Biol *116*, 817-825.
Kajita, M., Itoh, Y., Chiba, T., Mori, H., Okada, A., Kinoh, H., and Seiki, M. (2001). Membrane-type 1 matrix metalloproteinase cleaves CD44 and promotes cell migration. J Cell Biol *153*, 893-904.
Kawano, Y., Okamoto, I., Murakami, D., Itoh, H., Yoshida, M., Ueda, S., and Saya, H. (2000). Ras oncoprotein induces CD44 cleavage through phosphoinositide 3-OH kinase and the rho family of small G proteins. J Biol Chem *275*, 29628-29635.
Keane, M., Craig, T., Alfoldi, J., Berlin, A.M., Johnson, J., Seluanov, A., Gorbunova, V., Di Palma, F., Lindblad-Toh, K., Church, G.M.*, et al.* (2014). The Naked Mole Rat Genome Resource: facilitating analyses of cancer and longevity-related adaptations. Bioinformatics *30*, 3558-3560.
Kolliopoulos, C., Chatzopoulos, A., Skandalis, S.S., Heldin, C.H., and Heldin, P. (2021). TRAF4/6 Is Needed for CD44 Cleavage and Migration via RAC1 Activation. Cancers (Basel) *13*.
Koochekpour, S., Pilkington, G.J., and Merzak, A. (1995). Hyaluronic acid/CD44H interaction induces cell detachment and stimulates migration and invasion of human glioma cells in vitro. Int J Cancer *63*, 450-454.
Kung, C.I., Chen, C.Y., Yang, C.C., Lin, C.Y., Chen, T.H., and Wang, H.S. (2012). Enhanced membrane-type 1 matrix metalloproteinase expression by hyaluronan oligosaccharides in breast cancer cells facilitates CD44 cleavage and tumor cell migration. Oncol Rep *28*, 1808-1814.
Lee, S.B., Schramme, A., Doberstein, K., Dummer, R., Abdel-Bakky, M.S., Keller, S., Altevogt, P., Oh, S.T., Reichrath, J., Oxmann, D.*, et al.* (2010). ADAM10 is upregulated in melanoma metastasis compared with primary melanoma. J Invest Dermatol *130*, 763-773.
Lesley, J., and Hyman, R. (1998). CD44 structure and function. Front Biosci *3*, d616-630.
Leung, E.L., Fiscus, R.R., Tung, J.W., Tin, V.P., Cheng, L.C., Sihoe, A.D., Fink, L.M., Ma, Y., and Wong, M.P. (2010). Non-small cell lung cancer cells expressing CD44 are enriched for stem cell-like properties. PLoS One *5*, e14062.

Lokeshwar, B.L., Lokeshwar, V.B., and Block, N.L. (1995). Expression of CD44 in prostate cancer cells: association with cell proliferation and invasive potential. Anticancer Res *15*, 1191-1198.
Ludwig, A., Hundhausen, C., Lambert, M.H., Broadway, N., Andrews, R.C., Bickett, D.M., Leesnitzer, M.A., and Becherer, J.D. (2005). Metalloproteinase inhibitors for the disintegrin-like metalloproteinases ADAM10 and ADAM17 that differentially block constitutive and phorbol ester-inducible shedding of cell surface molecules. Comb Chem High Throughput Screen *8*, 161-171.
Ludwig, N., Szczepanski, M.J., Gluszko, A., Szafarowski, T., Azambuja, J.H., Dolg, L., Gellrich, N.C., Kampmann, A., Whiteside, T.L., and Zimmerer, R.M. (2019). CD44(+) tumor cells promote early angiogenesis in head and neck squamous cell carcinoma. Cancer Lett *467*, 85-95.
Marcello, E., Borroni, B., Pelucchi, S., Gardoni, F., and Di Luca, M. (2017). ADAM10 as a therapeutic target for brain diseases: from developmental disorders to Alzheimer's disease. Expert Opin Ther Targets *21*, 1017-1026.
Maretzky, T., Evers, A., Le Gall, S., Alabi, R.O., Speck, N., Reiss, K., and Blobel, C.P. (2015). The cytoplasmic domain of a disintegrin and metalloproteinase 10 (ADAM10) regulates its constitutive activity but is dispensable for stimulated ADAM10-dependent shedding. J Biol Chem *290*, 7416-7425.
Maretzky, T., Reiss, K., Ludwig, A., Buchholz, J., Scholz, F., Proksch, E., de Strooper, B., Hartmann, D., and Saftig, P. (2005). ADAM10 mediates E-cadherin shedding and regulates epithelial cell-cell adhesion, migration, and beta-catenin translocation. Proc Natl Acad Sci U S A *102*, 9182-9187.
Masson, D., Denis, M.G., Denis, M., Blanchard, D., Loirat, M.J., Cassagnau, E., and Lustenberger, P. (1999). Soluble CD44: quantification and molecular repartition in plasma of patients with colorectal cancer. Br J Cancer *80*, 1995-2000.
Matthews, V., Schuster, B., Schutze, S., Bussmeyer, I., Ludwig, A., Hundhausen, C., Sadowski, T., Saftig, P., Hartmann, D., Kallen, K.J.*, et al.* (2003). Cellular cholesterol depletion triggers shedding of the human interleukin-6 receptor by ADAM10 and ADAM17 (TACE). J Biol Chem *278*, 38829-38839.
Miletti-Gonzalez, K.E., Murphy, K., Kumaran, M.N., Ravindranath, A.K., Wernyj, R.P., Kaur, S., Miles, G.D., Lim, E., Chan, R., Chekmareva, M.*, et al.* (2012). Identification of function for CD44 intracytoplasmic domain (CD44-ICD): modulation of matrix metalloproteinase 9 (MMP-9) transcription via novel promoter response element. J Biol Chem *287*, 18995-19007.
Murai, T., Miyauchi, T., Yanagida, T., and Sako, Y. (2006). Epidermal growth factor-regulated activation of Rac GTPase enhances CD44 cleavage by metalloproteinase disintegrin ADAM10. Biochem J *395*, 65-71.
Murai, T., Miyazaki, Y., Nishinakamura, H., Sugahara, K.N., Miyauchi, T., Sako, Y., Yanagida, T., and Miyasaka, M. (2004). Engagement of CD44 promotes Rac activation and CD44 cleavage during tumor cell migration. J Biol Chem *279*, 4541-4550.
Murakami, D., Okamoto, I., Nagano, O., Kawano, Y., Tomita, T., Iwatsubo, T., De Strooper, B., Yumoto, E., and Saya, H. (2003). Presenilin-dependent gamma-secretase activity mediates the intramembranous cleavage of CD44. Oncogene *22*, 1511-1516.
Murphy, G. (2008). The ADAMs: signalling scissors in the tumour microenvironment. Nat Rev Cancer *8*, 929-941.
Nagano, O., Murakami, D., Hartmann, D., De Strooper, B., Saftig, P., Iwatsubo, T., Nakajima, M., Shinohara, M., and Saya, H. (2004). Cell-matrix interaction via CD44 is independently regulated by different metalloproteinases activated in response to extracellular Ca(2+) influx and PKC activation. J Cell Biol *165*, 893-902.
Nagano, O., and Saya, H. (2004). Mechanism and biological significance of CD44 cleavage. Cancer Sci *95*, 930-935.
Nakamura, H., Suenaga, N., Taniwaki, K., Matsuki, H., Yonezawa, K., Fujii, M., Okada, Y., and Seiki, M. (2004). Constitutive and induced CD44 shedding by ADAM-like proteases and membrane-type 1 matrix metalloproteinase. Cancer Res *64*, 876-882.

Oka, K., Fujioka, S., Kawamura, Y., Komohara, Y., Chujo, T., Sekiguchi, K., Yamamura, Y., Oiwa, Y., Omamiuda-Ishikawa, N., Komaki, S.*, et al.* (2022). Resistance to chemical carcinogenesis induction via a dampened inflammatory response in naked mole-rats. Commun Biol *5*, 287.

Okamoto, I., Kawano, Y., Matsumoto, M., Suga, M., Kaibuchi, K., Ando, M., and Saya, H. (1999a). Regulated CD44 cleavage under the control of protein kinase C, calcium influx, and the Rho family of small G proteins. J Biol Chem *274*, 25525-25534.

Okamoto, I., Kawano, Y., Murakami, D., Sasayama, T., Araki, N., Miki, T., Wong, A.J., and Saya, H. (2001). Proteolytic release of CD44 intracellular domain and its role in the CD44 signaling pathway. J Cell Biol *155*, 755-762.

Okamoto, I., Kawano, Y., Tsuiki, H., Sasaki, J., Nakao, M., Matsumoto, M., Suga, M., Ando, M., Nakajima, M., and Saya, H. (1999b). CD44 cleavage induced by a membrane-associated metalloprotease plays a critical role in tumor cell migration. Oncogene *18*, 1435-1446.

Okamoto, I., Tsuiki, H., Kenyon, L.C., Godwin, A.K., Emlet, D.R., Holgado-Madruga, M., Lanham, I.S., Joynes, C.J., Vo, K.T., Guha, A.*, et al.* (2002). Proteolytic cleavage of the CD44 adhesion molecule in multiple human tumors. Am J Pathol *160*, 441-447.

Olsson, E., Honeth, G., Bendahl, P.O., Saal, L.H., Gruvberger-Saal, S., Ringner, M., Vallon-Christersson, J., Jonsson, G., Holm, K., Lovgren, K.*, et al.* (2011). CD44 isoforms are heterogeneously expressed in breast cancer and correlate with tumor subtypes and cancer stem cell markers. BMC Cancer *11*, 418.

Omerbasic, D., Smith, E.S., Moroni, M., Homfeld, J., Eigenbrod, O., Bennett, N.C., Reznick, J., Faulkes, C.G., Selbach, M., and Lewin, G.R. (2016). Hypofunctional TrkA Accounts for the Absence of Pain Sensitization in the African Naked Mole-Rat. Cell Rep *17*, 748-758.

Pan, Y., Han, C., Wang, C., Hu, G., Luo, C., Gan, X., Zhang, F., Lu, Y., and Ding, X. (2012). ADAM10 promotes pituitary adenoma cell migration by regulating cleavage of CD44 and L1. J Mol Endocrinol *49*, 21-33.

Radotra, B., McCormick, D., and Crockard, A. (1994). CD44 plays a role in adhesive interactions between glioma cells and extracellular matrix components. Neuropathol Appl Neurobiol *20*, 399-405.

Reiss, K., and Bhakdi, S. (2012). Pore-forming bacterial toxins and antimicrobial peptides as modulators of ADAM function. Med Microbiol Immunol *201*, 419-426.

Reiss, K., Maretzky, T., Ludwig, A., Tousseyn, T., de Strooper, B., Hartmann, D., and Saftig, P. (2005). ADAM10 cleavage of N-cadherin and regulation of cell-cell adhesion and beta-catenin nuclear signalling. EMBO J *24*, 742-752.

Reiss, K., and Saftig, P. (2009). The "a disintegrin and metalloprotease" (ADAM) family of sheddases: physiological and cellular functions. Semin Cell Dev Biol *20*, 126-137.

Ruby, J.G., Smith, M., and Buffenstein, R. (2018). Naked Mole-Rat mortality rates defy gompertzian laws by not increasing with age. Elife *7*.

Sahin, U., Weskamp, G., Kelly, K., Zhou, H.M., Higashiyama, S., Peschon, J., Hartmann, D., Saftig, P., and Blobel, C.P. (2004). Distinct roles for ADAM10 and ADAM17 in ectodomain shedding of six EGFR ligands. J Cell Biol *164*, 769-779.

Schultz, K., Grieger Lindner, C., Li, Y., Urbanek, P., Ruschel, A., Minnich, K., Bruder, D., Gereke, M., Sechi, A., and Herrlich, P. (2018). Gamma secretase dependent release of the CD44 cytoplasmic tail upregulates IFI16 in cd44-/- tumor cells, MEFs and macrophages. PLoS One *13*, e0207358.

Seluanov, A., Hine, C., Azpurua, J., Feigenson, M., Bozzella, M., Mao, Z., Catania, K.C., and Gorbunova, V. (2009). Hypersensitivity to contact inhibition provides a clue to cancer resistance of naked mole-rat. Proc Natl Acad Sci U S A *106*, 19352-19357.

Siney, E.J., Holden, A., Casselden, E., Bulstrode, H., Thomas, G.J., and Willaime-Morawek, S. (2017). Metalloproteinases ADAM10 and ADAM17 Mediate Migration and Differentiation in Glioblastoma Sphere-Forming Cells. Mol Neurobiol *54*, 3893-3905.

Sugahara, K.N., Murai, T., Nishinakamura, H., Kawashima, H., Saya, H., and Miyasaka, M. (2003). Hyaluronan oligosaccharides induce CD44 cleavage and promote cell migration in CD44-expressing tumor cells. J Biol Chem *278*, 32259-32265.

Takaishi, S., Okumura, T., Tu, S., Wang, S.S., Shibata, W., Vigneshwaran, R., Gordon, S.A., Shimada, Y., and Wang, T.C. (2009). Identification of gastric cancer stem cells using the cell surface marker CD44. Stem Cells *27*, 1006-1020.

Tian, X., Azpurua, J., Hine, C., Vaidya, A., Myakishev-Rempel, M., Ablaeva, J., Mao, Z., Nevo, E., Gorbunova, V., and Seluanov, A. (2013). High-molecular-mass hyaluronan mediates the cancer resistance of the naked mole rat. Nature *499*, 346-349.

Trerotola, M., Guerra, E., Ali, Z., Aloisi, A.L., Ceci, M., Simeone, P., Acciarito, A., Zanna, P., Vacca, G., D'Amore, A.*, et al.* (2021). Trop-2 cleavage by ADAM10 is an activator switch for cancer growth and metastasis. Neoplasia *23*, 415-428.

Wang, Y., Zhou, N., Li, P., Wu, H., Wang, Q., Gao, X., Wang, X., and Huang, J. (2019a). EphA8 acts as an oncogene and contributes to poor prognosis in gastric cancer via regulation of ADAM10. J Cell Physiol *234*, 20408-20419.

Wang, Z., Tang, Y., Xie, L., Huang, A., Xue, C., Gu, Z., Wang, K., and Zong, S. (2019b). The Prognostic and Clinical Value of CD44 in Colorectal Cancer: A Meta-Analysis. Front Oncol *9*, 309.

Weskamp, G., Ford, J.W., Sturgill, J., Martin, S., Docherty, A.J., Swendeman, S., Broadway, N., Hartmann, D., Saftig, P., Umland, S.*, et al.* (2006). ADAM10 is a principal 'sheddase' of the low-affinity immunoglobulin E receptor CD23. Nat Immunol *7*, 1293-1298.

Wolf, K.J., Shukla, P., Springer, K., Lee, S., Coombes, J.D., Choy, C.J., Kenny, S.J., Xu, K., and Kumar, S. (2020). A mode of cell adhesion and migration facilitated by CD44-dependent microtentacles. Proc Natl Acad Sci U S A *117*, 11432-11443.

Yae, T., Tsuchihashi, K., Ishimoto, T., Motohara, T., Yoshikawa, M., Yoshida, G.J., Wada, T., Masuko, T., Mogushi, K., Tanaka, H.*, et al.* (2012). Alternative splicing of CD44 mRNA by ESRP1 enhances lung colonization of metastatic cancer cell. Nat Commun *3*, 883.

Yamane, N., Tsujitani, S., Makino, M., Maeta, M., and Kaibara, N. (1999). Soluble CD44 variant 6 as a prognostic indicator in patients with colorectal cancer. Oncology *56*, 232-238.

Zen, K., Liu, D.Q., Guo, Y.L., Wang, C., Shan, J., Fang, M., Zhang, C.Y., and Liu, Y. (2008). CD44v4 is a major E-selectin ligand that mediates breast cancer cell transendothelial migration. PLoS One *3*, e1826.

Zoller, M. (1995). CD44: physiological expression of distinct isoforms as evidence for organ-specific metastasis formation. J Mol Med (Berl) *73*, 425-438.

Zoller, M. (2011). CD44: can a cancer-initiating cell profit from an abundantly expressed molecule? Nat Rev Cancer *11*, 254-267.